

A NAC-type transcription factor confers aluminium resistance by regulating cell wall-associated receptor kinase 1 and cell wall pectin

He Qiang Lou^{1,2}  | Wei Fan^{1,4} | Jian Feng Jin¹ | Jia Meng Xu¹ | Wei Wei Chen^{1,3} | Jian Li Yang¹  | Shao Jian Zheng¹ 

¹State Key Laboratory of Plant Physiology and Biochemistry, College of Life Sciences, Zhejiang University, Hangzhou, China

²State Key Laboratory of Subtropical Silviculture, Zhejiang A & F University, Hangzhou, China

³Institute of Life Sciences, College of Life and Environmental Sciences, Hangzhou Normal University, Hangzhou, China

⁴College of Resources and Environment, Yunnan Agricultural University, Kunming, China

Correspondence

Jian Li Yang, State Key Laboratory of Plant Physiology and Biochemistry, College of Life Sciences, Zhejiang University, Hangzhou 310058, China.
Email: yangjianli@zju.edu.cn

Funding information

111 Project; Chang Jiang Scholars Program, Grant/Award Number: J.L.Y.; Natural Science Foundation of China, Grant/Award Numbers: 31222049 and 31501827

Abstract

Transcriptional regulation is important for plants to respond to toxic effects of aluminium (Al). However, our current knowledge to these events is confined to a few transcription factors. Here, we functionally characterized a rice bean (*Vigna umbellata*) NAC-type transcription factor, VuNAR1, in terms of Al stress response. We demonstrated that rice bean VuNAR1 is a nuclear-localized transcriptional activator, whose expression was specifically upregulated by Al in roots but not in shoot. VuNAR1 overexpressing *Arabidopsis* plants exhibit improved Al resistance via Al exclusion. However, VuNAR1-mediated Al exclusion is independent of the function of known Al-resistant genes. Comparative transcriptomic analysis revealed that VuNAR1 specifically regulates the expression of genes associated with protein phosphorylation and cell wall modification in *Arabidopsis*. Transient expression assay demonstrated the direct transcriptional activation of cell wall-associated receptor kinase 1 (WAK1) by VuNAR1. Moreover, yeast one-hybrid assays and MEME motif searches identified a new VuNAR1-specific binding motif in the promoter of WAK1. Compared with wild-type *Arabidopsis* plants, VuNAR1 overexpressing plants have higher WAK1 expression and less pectin content. Taken together, our results suggest that VuNAR1 regulates Al resistance by regulating cell wall pectin metabolism via directly binding to the promoter of WAK1 and induce its expression.

KEYWORDS

aluminium stress, cell wall-associated receptor kinase, nutrients, signalling, transcriptome

1 | INTRODUCTION

Aluminium (Al) is the most abundant metal element in the earth's crust, but it is not bioactive at neutral and alkaline soils. However, the solubility of Al increases dramatically when soil pH drops below 5, which impedes plant root growth and development (Kochian,

1995). As acid soils occupy approximately 50% of potential arable lands worldwide, Al toxicity is a serious problem in agriculture (Uexküll & Mutert, 1995). Therefore, improving plant resistance to Al toxicity is an urgent target for food security in acidic soils where many developing countries and poor farmers reside.

It remains a matter of debate whether the Al toxicity stems primarily from apoplast or symplast. Because Al has strong affinity to electron donors, it may target multiple sites simultaneously at cellular

*He Qiang Lou and Wei Fan contributed equally to the present work.

levels (Ma, 2007; Zheng & Yang, 2005). Interestingly, Sivaguru et al. (2003) found that Al could rapidly induce organ-specific expression of WAK1 in *Arabidopsis*, which confers Al resistance. WAKs are plasma membrane receptors that are linked to the cell wall pectin and have a cytoplasmic protein kinase domain (Kohorn & Kohorn, 2012). Given the existence of a cell wall-plasmalemma-cytoskeleton continuum, it may be unnecessary for Al to enter into cytoplasm to trigger signals associated with toxicity or resistance (Horst, Schmohl, Kollmeier, & Sivaguru, 1999; Wyatt & Carpita, 1993). Additionally, WAK1 can bind to and interact with pectin (Decreux & Messiaen, 2005). Thus, it is interesting to investigate whether WAK1 modulates Al resistance by affecting cell wall pectin.

Plants have evolved different kinds of strategies to deal with Al toxicity in acid soils. One of the most well-documented mechanisms is secretion of Al-induced root organic acid anions, malate, citrate, and oxalate, to chelate Al apoplastically (Ryan, Delhaize, & Jones, 2001; Yang, Fan, & Zheng, 2019), thus protecting cell wall from Al binding. Aluminium-activated malate transporter (ALMT) and multi-drug and toxin compounds extrusion (MATE) are two transporter families responsible for Al-activated malate and citrate secretion, respectively (Delhaize, Ma, & Ryan, 2012; Kochian, Piñeros, Liu, & Magalhaes, 2015). In addition, mutant approaches have identified some ABC transporters associated with Al resistance. In rice and buckwheat, STAR1 and STAR2 form a complex transporter protein that transports UDP-Glu out of cells to protect cell wall from Al binding (Huang, Sherman, & Lempicki, 2009; Xu et al., 2019). Being the closest homologues of rice OsSTAR1 and OsSTAR2, respectively, AtSTAR1 and ALS3 are involved in *Arabidopsis* Al resistance (Huang, Yamaji, & Ma, 2010; Larsen, Geisler, Jones, Williams, & Cancel, 2005). However, the mechanism by which AtSTAR1 and ALS3 resist Al may differ from that in rice because the complex of AtSTAR1/ALS3 is not able to transport UDP-Glu (Dong et al., 2017). Both rice OsALS1 and *Arabidopsis* ALS1 are tonoplast-localized Al transporters that sequester Al into vacuoles for final detoxification (Huang, Yamaji, Chen, & Ma, 2012; Larsen, Cancel, Rounds, & Ochoa, 2007).

Despite the fact that organic acid anions and UDP-Glu could protect cell wall from Al binding, cell wall accumulates a substantial amount of Al due to its strong electronegativity. The primary cell wall is composed of cellulose, hemicellulose, pectin, and structural proteins (Cosgrove, 2005). Al could either bind to the negatively charged carboxyl groups of pectin (Eticha, Stass, & Horst, 2005; Yang et al., 2008) or adsorb to uncharged hemicelluloses (Yang et al., 2011a; Zhu et al., 2012). Binding of Al to pectin depends not only on pectin content but also on the degree of pectin methylation that is determined by PME activity. Yang et al. (2013) found that Al-induced root elongation inhibition was in accordance with the increased expression of eight PME genes and PME activity in rice root apex. In *Arabidopsis*, PME46 functions as a PME inhibitor to reduce Al binding to pectin (Geng et al., 2017). Zhu et al. (2012) reported that *xth31* mutants are more resistant to Al toxicity in comparison with wild-type (WT) plants by reducing Al binding to hemicelluloses. XTH17 has major endotransglucosylase activity and interacts with XTH31 to modulate

hemicellulose content, thereby modulating Al resistance (Zhu et al., 2014). However, it is unknown how Al regulates the expression of these genes. Recently, a member of Groucho/TUP1 family of transcriptional corepressors, LUH was reported to interact with SEUSS-LIKE2 (SLK2) to form a complex, which in concert with other factors suppresses *PME46* expression, thereby inhibiting PME enzyme activity (Geng et al., 2017).

We have previously identified early Al-responsive genes from root tip of rice bean, an Al-resistant leguminous species well adapted to acid soils (Fan et al., 2014). Out of upregulated genes, there are three genes that encode transcription factor (TF) proteins including VuSTOP1, a heat stress TF B-2b like and a NAC domain-containing protein 2 like (Fan et al., 2014). In addition to TF genes, a subset of genes associated with cell wall modification including those associated with pectin and hemicellulose metabolism was also identified. VuSTOP1 could bind to the *VuMATE1* promoter and regulate its expression (Fan et al., 2015). How other TFs playing roles in Al resistance have yet to be investigated.

NAC (NAM, ATAF, CUC) gene family encodes plant-specific TFs, and several members of NAC genes have been shown to be involved in plant abiotic and biotic stress responses (Nuruzzaman, Sharoni, & Kikuchi, 2013). The involvement of some NAC TFs in drought stress response has been reported (Thirumalaikumar et al., 2017). In acid soils, the ability of the plants to withstand drought stress may be strongly impeded by Al toxicity, thus, the NAC TFs involved in drought stress response possibly regulate Al resistance. In addition, some NAC TFs have been identified as key regulators of secondary cell wall biosynthesis in *Arabidopsis*. For example, AtNST1, AtNST2, and AtNST3 function as master switches in regulating secondary cell wall biosynthesis. AtNST1 and AtNST2 are necessary for anther dehiscence (Mitsuda, Seki, Shinozaki, & Ohme-Takagi, 2005), although AtNST1 and AtNST3 function as master switches of fibre cell differentiation in *Arabidopsis* (Mitsuda et al., 2007; Zhong, Demura, & Ye, 2006). In monocots, some rice and corn NST orthologs could restore the drooping phenotype of *nst1nst3* double mutants in *Arabidopsis* (Yoshida et al., 2013; Zhong et al., 2011). The OsSWN2 chimeric repressor alters secondary wall formation in rice (Yoshida et al., 2013). Chai et al. (2015) demonstrated that OsSWN1 regulates the expression of many secondary cell wall-related genes in rice, which include many brittle culm genes. These findings suggested that these types of NAC TFs act as specific transcriptional switches to regulate the biosynthesis of cell wall (Hussey, Mizrahi, Creux, & Myburg, 2013; Yamaguchi & Demura, 2010; Zhong et al., 2011).

In this study, we isolated a previously identified NAC domain-containing protein 2 like gene, which was renamed as VuNAR1 (for *Vigna umbellata* NAC-type Al Responsive1). Ectopic expression of VuNAR1 in *Arabidopsis* showed significantly improved Al resistance in transgenic plants. Transcriptome analysis revealed that WAK1 was significantly upregulated by the VuNAR1, which affects cell wall pectin content. Thus, our findings suggest that a NAC TF is involved in Al resistance by regulating cell wall pectin metabolism via induced WAK1 expression.

2 | MATERIALS AND METHODS

2.1 | Plant materials and growth conditions

Rice bean (*Vigna umbellata*) seeds were germinated and cultured following previous work (Fan et al., 2015). For the tissue-specific expression, seedlings were exposed to 0 or 25 μM Al for 8 hr. For the time-course experiment, seedlings were subjected to 25 μM AlCl_3 for 0, 0.5, 1, 2, 4, 8, 12, or 24 hr. For the dose-response experiment, seedlings were subjected to 0, 5, 10, 25, or 50 μM of AlCl_3 for 8 hr. For other treatments, the seedlings were exposed to nutrient solution (pH 4.5) containing 25 μM AlCl_3 , 10 μM LaCl_3 , or 0.5 μM CuCl_2 for 8 hr. All experiments were carried out in an environmentally controlled growth room with a 12 hr/30°C day and a 12 hr/22°C night regime, a light intensity of 300 $\mu\text{mol photons m}^{-2} \text{s}^{-1}$ and a relative humidity of 65%.

2.2 | Cloning of cDNA and promoter sequence of genes

5' and 3'-RACE were performed according to the manufacturer's protocol of SMART RACE cDNA Amplification kit (Clontech). The primers used for RACE amplification were listed in Table S1. Sequence alignment and phylogenetic analysis was performed using DNAMAN and Mega 7.0 software, respectively. The DNA sequences upstream of translation start codons of *VuNAR1* and *WAK1*-like gene in rice bean (*VuWAKL1*) were isolated using genome walker libraries constructed previously (Liu et al., 2013).

2.3 | qRT-PCR analysis

Total RNA was isolated from rice bean or *Arabidopsis* using the RNAprep pure Plant Kit (Tiangen). First-strand cDNA was synthesized from 1 μg of total RNA using SuperScript reverse transcriptase (Takara). Gene expression levels were determined by quantitative reverse transcription polymerase chain reaction (qRT-PCR) using SYBR Premix Ex Taq™ kit (Takara) on a LightCycler 480 machine (Roche Diagnostics, Indianapolis, IN, USA). The relative expression was normalized to the expression level of the internal control (*18S rRNA* for rice bean and *AtACTIN2* for *Arabidopsis*). The primer pairs of each gene were listed in Table S1. The reaction condition was 45 cycles of 95°C for 10 s, 56°C for 10 s, and 72°C for 20 s. The relative expression was calculated by formula $2^{-\Delta\Delta\text{Cp}}$. The experiment was performed with three biological and technical replications.

2.4 | Subcellular localization and GUS analysis of *VuNAR1*

The full-length cDNA (without stop codon) and promoter region of *VuNAR1* were ligated into the binary vector *35S::GFP* (modified from pCAMBIA1300) and pCAMBIA1301 (fusion to the GUS gene) vector, respectively (Table S1). The resultant *35S::VuNAR1::GFP* and *VuNAR1p::GUS* plasmid was introduced into *Agrobacterium*

tumefaciens strain GV3101 and transformed into *Arabidopsis* WT plants (Col-0) by *Agrobacterium*-mediated transformation (Clough & Bent, 1998). Homozygous T3 plants were used for GFP or GUS analysis. For transient assays, *35S::VuNAR1::GFP* plasmids were infiltrated into tobacco (*Nicotiana benthamiana*) leaves. GFP fluorescence was observed via confocal laser scanning microscopy (LSM710: Karl Zeiss). GUS staining was performed according to Jefferson, Kavanagh, and Bevan (1987).

2.5 | Transactivation activity assay in yeast

The transcription activation assay in yeast was performed using the Matchmaker Gold System (Clontech). Different regions of *VuNAR1* CDS were cloned into pGBKT7 vector. These plasmids and control pGBKT7 were introduced into yeast strain AH109 that carried the GAL4-responsive GAL1 promoter and HIS3 reporter gene and cultured on either SD-Trp or SD-Trp-His medium at 30°C for 3 days according to the manufacturer's manual. The primer sequences were listed in Table S1.

2.6 | Generation of *VuNAR1* overexpressed plants and Al tolerance evaluation

The *35S::VuNAR1* plasmid was constructed by amplifying the entire CDS of *VuNAR1* by PCR with primer pair (Table S1) and cloned into a modified pCAMBIA1300 vector. The resulting vector was introduced into *A. tumefaciens* strain GV3101. Transformation of *Arabidopsis* plants was carried out by floral dip method. Hygromycin-resistant T1 plants were grown for seed harvest, and the corresponding T2 seeds displaying a 3:1 ratio for hygromycin resistance were selected for collecting T3 seeds. T3 seeds displaying 100% resistance to hygromycin were used for the following experiments. Over 50 independent positive transgenic lines were checked for *VuNAR1* expression by PCR using the primers listed in Table S1. Two independent lines with high *VuNAR1* expression levels were chosen for the next experiments. For root growth analyses, *Arabidopsis* seeds were surface sterilized and germinated in plates containing 0.8% (w/v) agar and one-fifth strength Hoagland nutrient solution (pH 5.5). Seedlings with about 1-cm root length were removed from the agar plates and subjected to a nutrient solution consisting of one-thirtieth strength Hoagland nutrient solution without $\text{NH}_4\text{H}_2\text{PO}_4$ and 1 mM CaCl_2 in a growth chamber with a 12-hr light/12-hr dark cycle at 23°C. For Al treatment, seedlings were grown on the nutrient solution containing 0 or 4 μM AlCl_3 at pH 5.0 for 6 days. The solution was renewed every 2 days. Al sensitivity was evaluated by relative root growth expressed as (root elongation with Al treatment/root elongation without Al) \times 100.

2.7 | Al content measurement

Al content in root cell wall was measured as described (Xia, Yamaji, Kasai, & Ma, 2010). Two-week-old seedlings of both WT *Arabidopsis*

and two VuNAR1ox lines were exposed to one fifth Hoagland solution (pH 5.0 without P) containing 25 μM Al for 8 hr. After the treatment, the roots were excised after washing three times with 0.5 mM CaCl_2 and then centrifuged at 3,000g in a Ultra free-MC Centrifugal filter units (millipore) for 10 min at 4°C to remove apoplastic solution. The roots were then frozen at -80°C for 12 hr. After thawing, the samples were centrifuged at 20,600g for 10 min at room temperature to remove root-cell sap. Cell wall was obtained by washing with 70% ethanol three times. Al in cell wall was extracted by 2 N HCl for 24 hr with occasional shaking. For total Al determination, roots were harvested, weighted, and digested with HNO_3 . The Al content was determined by inductively coupled plasma-atomic emission spectrometry (ICP-AES; IRIS/AP optical emission spectrometer).

2.8 | Morin staining

Al accumulation in the *Arabidopsis* root tips was visualized by morin staining. Two-week-old seedlings were exposed one-fifth Hoagland solution (pH 5.0 without P) containing 25 μM Al for 8 hr, the excised roots were washed in 10 mM MES buffer (pH 5.5) for 5 min and then stained with 100 μM morin in the same buffer for 30 min. The roots were further washed twice in MES buffer for 5 min each. The images were obtained using a confocal microscope (LSM710, Karl Zeiss, Jena, Germany) at 488-nm excitation wavelength.

2.9 | RNA-seq analysis

RNA-seq analysis was performed by 1GENE company (Hangzhou, China). Two-week old seedlings of both the WT (Col-0) and the VuNAR1ox line were exposed to a one-fifth Hoagland solution (pH 5.0 without P) containing 0 or 25 μM AlCl_3 for 4 hr. Total RNA was isolated, and mRNA was enriched and fragmented into about 200 bp in length by mixed with fragmentation buffer. First-strand cDNA was synthesized from fragmented mRNA using random hexamer primer. The double-stranded cDNA was purified and end repaired. Finally, 3' end single nucleotide A addition was performed, and sequencing adaptors were ligated to the fragments. The available fragments were selected and then enriched by PCR amplification. The constructed libraries were qualified and quantified using an Agilent 2100 Bioanalyzer and the ABI StepOnePlus Real-Time PCR System and then sequenced via Illumina HiSeq 4000. The obtained raw reads were then cleaned by removing the low-quality reads and/or adaptor sequences. The clean reads were mapped to reference sequences using SOAPaligner/SOAP2 (Li et al., 2009). The gene expression levels were calculated using the reads per kilobase per million reads method according to Mortazavi, Williams, McCue, Schaeffer, and Wold (2008).

2.10 | Bioinformatics analysis

Analysis of gene ontology (GO) enriched categories and clusterization into functional groups by cellular component was performed using Cytoscape (Shannon et al., 2003; version 3.4) plugin ClueGO +

CluePedia (Bindea et al., 2009). GO biological process (GOBP) enrichment analysis was performed to compute p values that indicate the significance of each GOBP being represented by the genes using DAVID software (Huang et al., 2009).

2.11 | GFP signal reporter assay

Genomic DNA from *Arabidopsis* was used as the template for amplification of the promoter sequence for constructing the reporter plasmid containing *Pro_{WAK1}:WAK1-GFP* (Table S1). 35S::VuNAR1 plasmid was used as the effector plasmid. Plasmids were transformed into *A. tumefaciens* strain GV3101. Agrobacterial cells were infiltrated into leaves of *N. benthamiana* with infiltration buffer (10 mM MgCl_2 , 0.2 mM acetosyringone, and 10 mM MES, pH 5.6). GFP fluorescence was observed by a confocal laser scanning microscopy (LSM710, Karl Zeiss, Jena, Germany).

2.12 | Yeast one-hybrid assay

The yeast one-hybrid assay was performed using the MATCH-MAKER Gold Yeast One-Hybrid Library Screening System (Clontech) and YEASTMAKER Yeast Transformation System2 (Clontech). The open reading frame sequence of VuNAR1 and various promoter fragments of *AtWAK1* and *VuWAKL1* were amplified. Primer pairs used were listed in Table S1. The open reading frame of VuNAR1 described above was cloned in frame after transcriptional activation domain of yeast GAL4 TF (without DNA-binding domain) in pGADT7. The amplified various promoter fragments and annealed oligonucleotides were cloned upstream of the Aureobasidin A (AbA) resistance reporter gene (AUR1-C) in the pAbAi vector. Pairs of plasmids were introduced into yeast strain Y1H gold and cultured on SD medium without Leu containing 0 to 400 ng ml^{-1} AbA at 30°C for 3 days.

2.13 | Cell wall components extraction and determination

Crude cell wall and different cell wall components were extracted from *Arabidopsis* root according to Yang et al. (2011) with some modifications. Roots were ground in liquid nitrogen and then homogenized with 75% ethanol in ice bath for 20 min. After centrifuged at 8,000 rpm for 10 min, the supernatant of sample was removed. The pellets were resuspend with acetone, methanol:chloroform (1:1; v/v), and methanol, respectively, for 20 min each, with each supernatant being removed after centrifugation between the washes. The remaining pellet was freeze-dried and stored at 4°C as crude cell wall. Pectin was extracted twice by hot water for 1 hr each, and the supernatants were combined for pectin determination. Pectin content was spectrophotometrically measured at 520 nm using galacturonic acid as standard (Blumenkrantz & Asboe-Hansen, 1973). The remaining pellets were then extracted twice with 4% (w/v) KOH containing 0.02% (w/v) KBH_4 at room temperature for a total time of 24 hr and the supernatants were combined for hemicelluloses 1 determination. The resulting

pellet was subsequently extracted twice with a solution containing 24% (w/v) KOH and 0.02% (w/v) KBH_4 for 24 hr and the combined supernatant was used for hemicellulose 2 determination. Total polysaccharide content was used to indicate hemicelluloses content, which was spectrophotometrically measured at 490 nm using glucose as standard.

3 | RESULTS

3.1 | Isolation and phylogenetic analysis of VuNAR1

We previously identified an expression sequence tag homologous to a NAC-type TF whose expression was upregulated by Al stress in root tip of rice bean (Fan et al., 2014). On the basis of rapid amplification of cDNA ends (RACE)-PCR method, we isolated the full-length cDNA of VuNAR1 (GenBank accession no. MG256389). The VuNAR1 coding region is 861 bp in length and encodes a protein of 287 amino acids. BLAST searches revealed that the closest homologue of VuNAR1 is ATAF1 in *Arabidopsis*, sharing 58% identity in the deduced amino acid sequence. Interestingly, we found that the C-terminal regions are variable between VuNAR1 and ATAF1, though they have highly conserved NAC DNA binding domain (Figure S1a). Phylogenetic analysis showed that VuNAR1 with some members from *Fabaceae* is clustered into a distinct clade, but ATAF1 is clustered with those from both monocots and dicots (Figure S1b), implying that VuNAR1 may have specific roles different from *Arabidopsis* ATAF1.

3.2 | Expression patterns of VuNAR1

qRT-PCR analysis revealed that VuNAR1 was expressed at root tip, basal roots, and leaves of rice bean at seedlings stage (Figure 1a). When seedlings were exposed to Al, the expression of VuNAR1 was increased at both root tip and basal root regions but not in leaves (Figure 1a). A time-course experiment showed that the expression was induced by Al as early as a half hour and reached the plateau at 2 hr of exposure. However, the expression decreased to a level similar to that without Al after 8 hr of exposure (Figure 1b). The expression of VuNAR1 increased with increasing Al concentrations, though there was no significant difference between 0 and 5 μM Al concentrations (Figure 1c). The expression of VuNAR1 did not respond to low pH and other metals including lanthanum and copper (Figure 1d), indicating that VuNAR1 responds to Al stress specifically.

We further investigated the expression pattern of VuNAR1 through VuNAR1 promoter-GUS reporter assays in *Arabidopsis*. A 1546-bp DNA sequence upstream of the translation start codon was isolated (Figure S2), fused to a GUS reporter gene, and transformed into *Arabidopsis* WT plants. In the absence of Al, GUS activity was observed throughout 7-day-old *Arabidopsis* seedlings (Figure 1e). Al stress resulted in the increase of GUS activity in roots but not in shoots (Figure 1f). In root tip, GUS activity was strongly expressed at root cap, transition zone between elongation zone and meristem, and elongation zone, but weakly at meristem (Figure 1g). Al dramatically increased GUS activity throughout the entire root tip region (Figure 1h).

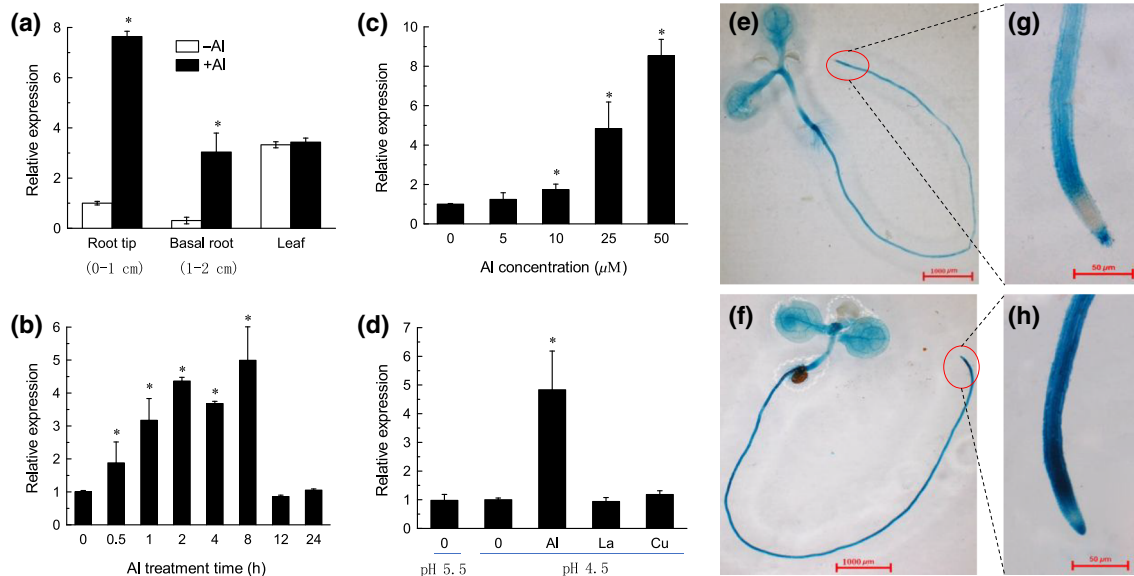


FIGURE 1 Expression pattern of VuNAR1. (a) Expression of VuNAR1 in rice bean root apices (0–1 cm), basal roots (1–2 cm), and leaves in the absence or presence of Al stress. (b) Time-dependent expression of VuNAR1 in rice bean root apices (0–1 cm) in response to 25 μM Al for different times. (c) Dose response of VuNAR1 in rice bean root apices (0–1 cm) exposed for 8 hr to different concentrations of Al. (d) Relative expression of VuNAR1 in rice bean root apices (0–1 cm) in response to low pH (pH 4.5) and LaCl_3 (10 μM) or CuCl_2 (0.5 μM) at pH 4.5 conditions. Al (25 μM) was included as a reference. Three-day-old seedlings were exposed to different treatments. Data are expressed as means \pm SD ($n = 3$). 18S rRNA was used as internal control. Asterisks are significantly different between treatments at $p < .05$. (e) to (h), VuNAR1p::GUS expression analysis in transgenic *Arabidopsis* plants. (e) and (f), whole seedlings. (g) and (h) root apex. Transgenic seedlings were exposed to 1/30 Hoagland nutrient solution without (e and g) or with (f and h) 10 μM Al at pH 5.0 for 8 hr. At least two independent transgenic lines were used to analyse the GUS activity. Bar = 1 mm in e and f; 50 μm in g and h

3.3 | VuNAR1 is a nuclear-localized TF

To examine whether VuNAR1 has transcriptional activation potential, we first investigated the subcellular localization of VuNAR1. We constructed transgenic *Arabidopsis* plants overexpressing either a VuNAR1-GFP fusion protein or GFP protein alone under the control of the cauliflower mosaic virus (CaMV) 35S promoter. Although GFP protein alone was found to be present at both cytoplasm and nucleus of transgenic *Arabidopsis* roots, VuNAR1-GFP fusion protein was present exclusively at nucleus (Figure 2a). To further examine the nuclear localization of VuNAR1, the subcellular localization of VuNAR1 was determined in a transient expression system in *N. benthamiana* leaves. The VuNAR1-GFP fusion protein was found to be exclusively present at the nuclei of these leaves, whereas GFP protein alone was present at both cytoplasm and nuclei (Figure 2b). When VuNAR1-GFP protein was coexpressed with OsART1-RFP that was a nuclear-localized TF (Yamaji et al., 2009), they were colocalized. These results indicate that VuNAR1 localizes in cell nuclei.

We then examined the transactivation potential of VuNAR1 using a yeast expression system. Yeast strain AH109 was transformed with plasmid carrying the DNA-binding domain of the yeast GAL4 TF (DB_{GAL4}) fused with different fragments of VuNAR1 protein

(Figure 2c). Yeast cells carrying DB_{GAL4} -VuNAR1-full (plasmid A) grew well in SD medium lacking His, whereas cells carrying DB_{GAL4} alone (plasmid E) did not. To further examine which region of VuNAR1 is responsible for the transactivation, we segmented the VuNAR1 further into 1–158 aa (plasmid B), 7–158 aa (plasmid C), and 159–287 aa (plasmid D). Although yeast cells carrying plasmid D grew as well as plasmid A, others did not, suggesting that it is the variable C-terminal region that has transactivation potential. In the presence of X-gal in the growth medium, yeast cells that grew well on the SD medium without His turned blue, suggesting that the expression of a second reporter gene, *LacZ*, was also activated (Figure 2d).

3.4 | Overexpression of VuNAR1 in *Arabidopsis* confers AI resistance

To gain insight into the role of VuNAR1 in AI resistance, we carried out ectopic expression of VuNAR1 in *Arabidopsis*. RT-PCR analysis showed that VuNAR1 was highly expressed in two independent transgenic lines (line1 and line2) but not in plants carrying empty vector (Figure 3a). In the absence of AI, line1 and line2 showed slightly increased root elongation in comparison with WT plants (Figure 3b).

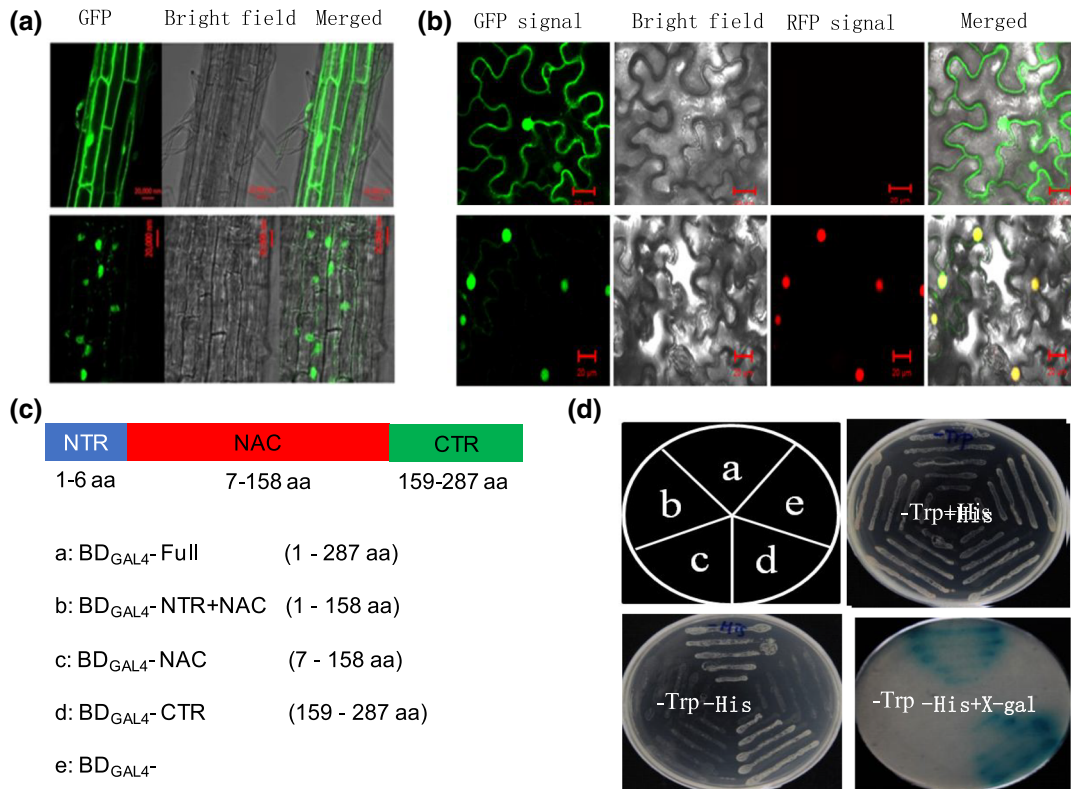


FIGURE 2 Localization and transcriptional activation analysis of VuNAR1. (a) Subcellular localization of VuNAR1 in transgenic *Arabidopsis* roots. 35S:VuNAR1-GFP construct was introduced into *Arabidopsis* plants. The homozygous T3 seedlings were used to observe GFP fluorescence, bar = 20 μ m. (b) Subcellular localization of VuNAR1 in *Nicotiana benthamiana* leaves. Upper panel: 35S:GFP plasmid was transformed into *N. benthamiana* leaves. Lower panel: both 35S:VuNAR1-GFP and 35S:OsART1-RFP constructs were transiently coexpressed in *N. benthamiana* leaves, bar = 20 μ m. (c) Schematic representation of the constructs used for transcriptional activation assay in yeast. VuNAR1 was truncated to generate four fragments including that encodes full-length cDNA. (d) Transcriptional activation assay in yeast

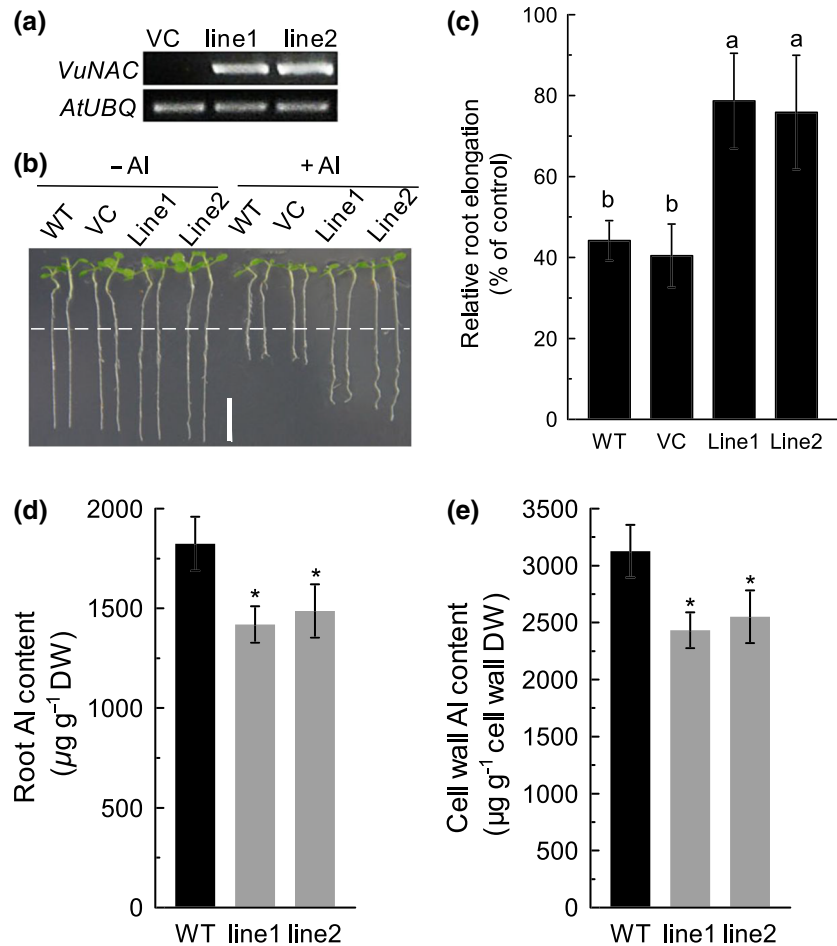


FIGURE 3 Overexpression of VuNAR1 enhances Al resistance in *Arabidopsis* via Al exclusion. (A) reverse transcription polymerase chain reaction characterization of VuNAR1 expression in two independent transgenic lines (line1 and line2). (b) Root growth of wild-type (WT), vector control (VC), and VuNAR1 overexpressing lines. Seven-day-old seedlings with 1-cm root length were transferred to 1/30 Hoagland nutrient solution (without NH₄H₂PO₄ and 1 mM CaCl₂) containing either 0 or 4 µM Al for 6 days, bar = 1 cm. (c) Relative primary root growth of WT, VC, and VuNAR1 overexpressing lines. Data are means ± SD (*n* = 20). Columns with different letters are significantly different at *p* < .05. (d) Total root Al content. (e) Cell wall Al content. Two-week-old seedlings were exposed to one-fifth Hoagland solution (pH 5.0 without P) containing 25 µM Al for 8 hr. Data are means ± SD (*n* = 4). Asterisks are significantly different between treatments at *p* < .05

Although Al stress inhibited root elongation by 60% in both WT and empty vector controls, only 20% inhibition was observed in both transgenic lines (Figure 3c).

To understand whether Al exclusion or internal tolerance mechanism is involved in VuNAR1-mediated Al resistance in *Arabidopsis* plants, we analysed total root Al content and cell wall Al content. Compared with WT plants, the total Al content of roots were 22% and 18% lower in line1 and line2, respectively (Figure 3d). In addition, a lower intensity of morin staining (which stains Al) in the root of transgenic lines after a 4-hr exposure to 25 µM Al (Figure S3) were also observed. These results suggest that VuNAR1 could reduce Al accumulation in the root of transgenic lines. Further analysis revealed that cell wall Al content was significantly reduced in both transgenic lines, which were 21% lower in line1 and 18% lower in line2 than that of WT (Figure 3e). These results suggest that VuNAR1 may confer Al resistance by reducing Al bound to cell walls.

To check whether VuNAR1 is a functional homologue of ATAF1, we investigated the Al resistance of *ataf1* mutant. Although the expression of ATAF1 was upregulated by Al stress (Figure S4), there was no difference between WT and *ataf1* mutants with respect to root growth either in the absence or presence of Al stress, showing similar relative root elongation (Figure S5). Then, we investigated the role of ATAF1 in Al resistance by overexpressing ATAF1 in *Arabidopsis* (ATAF1ox). Interestingly, the ATAF1ox line displayed retarded growth

in the absence of stress in comparison with WT plants, which was in accordance with previous report (Wu et al., 2009). Moreover, there was no difference in Al resistance between ATAF1ox and WT. These results suggest that VuNAR1 is functionally different from ATAF1 in terms of Al resistance.

3.5 | Known genes involved in Al exclusion are not related to enhanced Al resistance

STOP1 is the master TF that controls Al resistance in *Arabidopsis* by regulating the major Al resistance gene *AtALMT1* and *AtMATE* expression (Iuchi et al., 2007; Liu, Magalhaes, Shaff, & Kochian, 2009). In addition, STOP2 and CAMTA2 have also been reported to play a positive role in regulating *AtALMT1* expression (Kobayashi et al., 2014; Tokizawa et al., 2015). To examine whether VuNAR1-mediated Al exclusion is associated with known Al resistance mechanisms, we carried out qRT-PCR analysis of these known Al resistance gene expression in WT and VuNAR1 overexpressing line1 (OX hereafter). The expression of STOP1 and STOP2 was not affected significantly by Al stress, but CAMTA2 was induced (Figure 4a). However, there were no significant differences between WT and OX plants (Figure 4a). Differences in the expression induction of both *AtALMT1* and *AtMATE* between WT and OX plants were also not observed (Figure 4b).

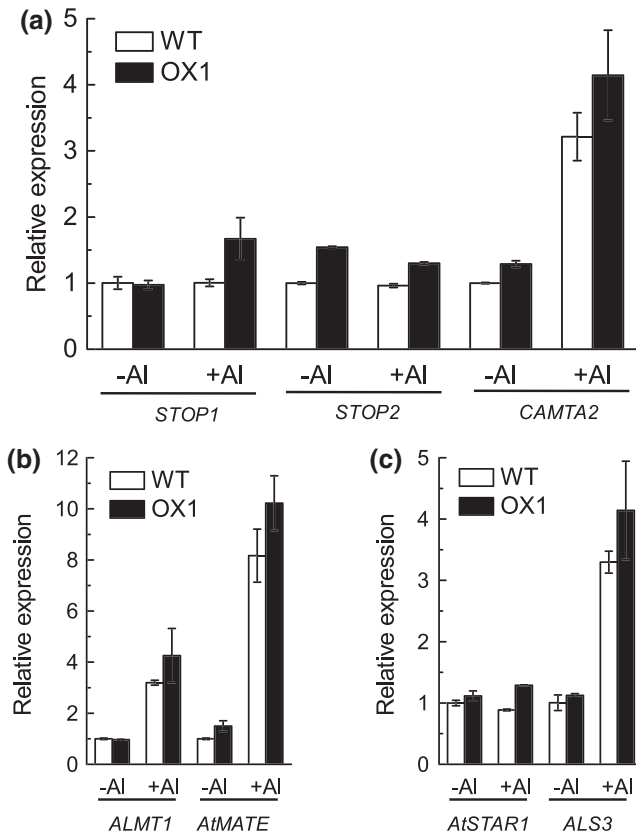


FIGURE 4 Quantitative reverse transcription polymerase chain reaction analysis of genes involved in external exclusion of Al. (a) Expression of transcription factor genes that are involved in expression regulation of *ALMT1* and *AtMATE*. (b) Expression of *ALMT1* and *AtMATE*. (c) Expression of *AtSTAR1* and *ALS3*. Two-week-old seedlings were exposed to one-fifth Hoagland solution (pH 5.0 without P) containing 25 μ M for 4 hr. *AtACTIN2* was used as the internal reference. Data are means \pm SD ($n = 3$)

To verify whether increased Al resistance in OX plants is associated with the regulation of *AtSTAR1* and *ALS3* expression, we further compared their expression between WT and OX plants. While *ALS3* expression was greatly induced by Al stress, *AtSTAR1* was constitutively expressed (Figure 4C), which is in accordance with previous results (Sawaki et al., 2009; Huang et al., 2010). However, there was no difference in the expression between WT and OX plants either in the absence or in the presence of Al (Figure 4C), suggesting that neither *AtSTAR1* nor *ALS3* is involved in VuNAR1-mediated Al resistance.

3.6 | Differential expression analysis revealed apoplastic regulation of Al resistance

To understand how VuNAR1 mediates Al resistance in *Arabidopsis*, we performed a comparative RNA sequencing (RNA-seq) analysis of gene expression in roots from WT and OX plants grown under -Al (0 μ M Al, 4 hr) and +Al conditions (10 μ M Al, 4 hr). For this experiment, seedlings were cultured hydroponically with or without 25 μ M Al for 4

hr. The difference of expression level between two samples is determined as $\log_2FC > 1.0$ and false discovery rate < 0.05 . Compared with WT roots without Al (WT -Al), the expression was induced for 903 genes and was repressed for 604 genes in the WT roots treated with Al (WT +Al), and that was induced for 686 genes and repressed for 498 genes in OX roots treated with Al (OX +Al; Figure 5a). In the absence of Al, a total of 345 genes (247 up; 98 down) were changed in OX in comparison with WT (OX -A; Figure 5a). Only 110 genes (44 up; 66 down) were found to be specifically expressed in OX +Al roots (Figure 5a).

To obtain a global overview of the differential response to Al stress between WT and OX, we first performed a GO enrichment analysis of cellular component between WT and OX plants (Figure 5b). In WT roots, we found five most significantly enriched categories of cellular component and included intracellular organelle (GO:0043229), cell periphery (GO:0071944), anchored component of membrane (GO:0031225), cell wall (GO:0005618), and intrinsic component of membrane (GO:0031224). By contrast, in OX roots, they are cell periphery (GO:0071944), cell wall (GO:0005618), anchored component of membrane (GO:0031225), intrinsic component of membrane (GO:0031224), and intrinsic component of plasma membrane (GO:0031226). These results suggest that overexpression of VuNAR1 protects OX plant roots from symplastic lesions of Al. A full list of the GO categories that were enriched is included in Table S2.

We then performed a GOBP analysis of 110 OX-specific genes under +Al conditions (Table S2). To systemically explore the VuNAR1-mediated Al resistance, the VuNAR1-induced or repressed genes were separately subjected to GOBP analysis (Figure 5c). Remarkably, the genes in the upregulated group are mainly involved in protein phosphorylation (GO:0006468) and transmembrane receptor protein tyrosine kinase signalling pathway (GO:0007169). Intriguingly, we found that a gene encoding wall-associated kinase, *WAK1*, was upregulated by VuNAR1 and included in GOBP of protein phosphorylation (Figure 5d). By contrast, the genes in the downregulated group are mainly involved in plant-type cell wall organization (GO:0009664) and pectin catabolic process (GO:0045490).

To confirm the data from the RNA-seq, the transcription of 18 genes was analysed using qRT-PCR. The correlation between the RNAseq and qRT-PCR data was highly significant ($r = .736$, $p < .001$; Figure S6).

3.7 | VuNAR1 binds to the *WAK1* and *VuWAKL1* promoters in vivo

The increased expression of *WAK1* in VuNAR1 overexpressing lines promoted us to test whether VuNAR1 binds to the promoter of *WAK1*, thereby activating its transcription. To test this possibility, we introduced a 1882-bp length sequence of *WAK1* promoter fused with CaMV 35S minimal (-46) promoter and *GFP* as a reporter gene into tobacco leaves. As an effector, either VuNAR1 cDNA under the control of CaMV 35S promoter or the vector control was coexpressed

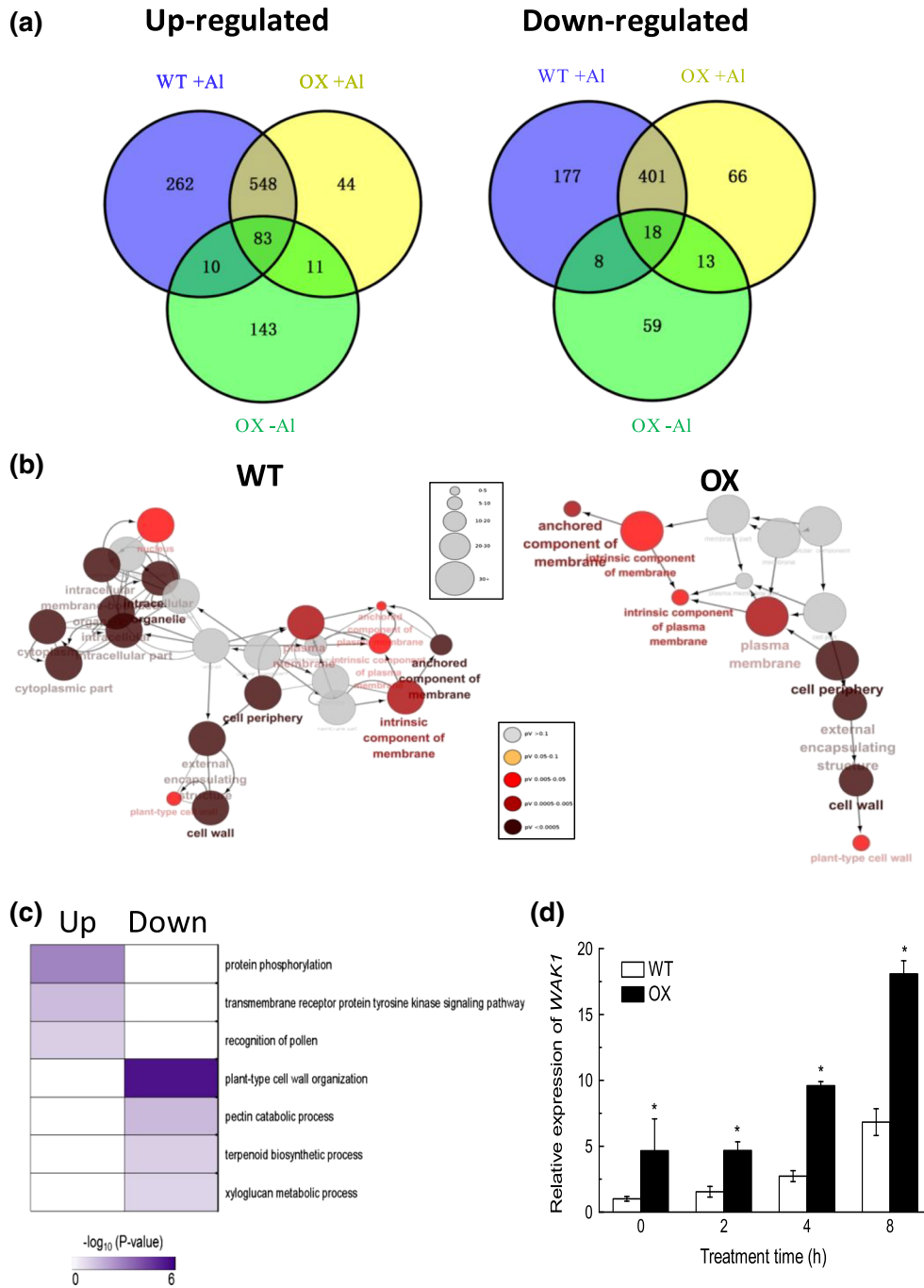


FIGURE 5 RNA-seq analyses of differential expressed genes in the roots of wild-type (WT) and VuNAR1 overexpressing line1 (OX). (a) Venn diagram of differential expressed genes that are upregulate and downregulated, $-1.0 > \log_2FC(+AI/-AI) > 1.0$; false discovery rate < 0.05 . WT -AI condition was used as the control for the comparisons of differential expression. (b) Gene ontology (GO) enrichment analysis of cellular component that are activated by AI stress in WT and OX plant roots. Each circle corresponds to an enriched GO cellular component. Colour code represents p value (hypergeometric test; Benjamini-Hochberg correction) and size represents the number of genes that are associated with respective GO category. GO categories that share genes are connected and clustered by the cellular component that corresponds to the most significantly enriched category of the cluster. (c) GO biological processes enriched by the genes that are specifically upregulated and downregulated by VuNAR1. The colour bar represents the gradient of $-\log_{10}(P)$, where P is the enrichment of a p value computed by DAVID. (d) Quantitative reverse transcription polymerase chain reaction analysis of WAK1. Seedlings of *Arabidopsis*, WT, and OX were exposed to 2-week-old seedlings that were exposed to one-fifth Hoagland solution (pH 5.0 without P) containing 25 μ M AI for different times. Data are expressed as means \pm SD ($n = 3$). Asterisks are significantly different between genotypes at $p < .05$

(Figure 6a). In comparison with vector control, the presence of VuNAR1 effector dramatically enhanced the GFP signals, suggesting that VuNAR1 activates WAK1 expression in vivo (Figure 6b).

To further verify whether VuNAR1 regulates WAK1 by directly binding to its promoter, we used the yeast one-hybrid approach. We separated a 1882-bp DNA sequence upstream of WAK1 start codon

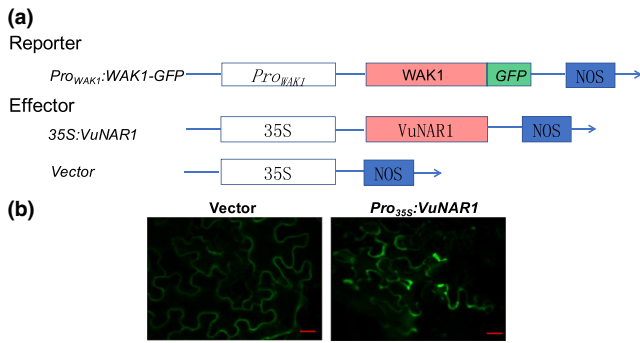


FIGURE 6 Transient assay of WAK1 expression by VuNAR1. (a) Schematic representation of the constructs used for transient expression assays. The reporter construct consists of a WAK1 promoter, WAK1 gene fused with the GFP coding sequence, and a NOS terminator. Effector constructs express VuNAC under the control of the cauliflower mosaic virus 35S promoter. (b) VuNAC activates the promoter of WAK1 and regulates the expression of WAK1 in transient expression assays

into five parts, P1 (−1 to −299), P2 (−300 to −651), P3 (−632 to −947), P4 (−928 to −1,410), and P5 (−1,392 to −1,882; Figure 7a) and introduced individually into the pAbAi vector that contains the AbA resistance reporter gene (*AUR1-C*). The VuNAR1 cDNA was cloned in frame after the transcription activation domain of the yeast TF GAL4

into pGADT7. In the absence of AbA, all yeast cells grew well. In the presence of AbA, yeast cells containing P2, P4, or P5 could grow, but those containing P1 or P3 could not, suggesting that VuNAR1 could bind to P2, P4, and P5 of WAK1 promoter to activate *AUR1-C* expression in yeast (Figure 7b).

NAC TFs recognize the consensus *cis*-acting elements, CGT(G/A) and CACG, or NAC recognition sequences (NACRSs; Simpson et al., 2003; Tran et al., 2004). Our search for such potential *cis*-elements revealed that there is at least one motif in all five regions except P2, suggesting that VuNAR1 may bind a novel motif (Figure 7a). To find the specific binding motif conserved among P2, P4, and P5, we used the MEME motif discovery tool (<http://meme-suite.org>). We identified an 9-bp consensus sequence that contains an ABA responsive *cis*-element, CA(A/C/T)GTA (Figure 7c).

To check the importance of this ABA responsive *cis*-element (hereafter termed VuNAR1BM) for VuNAR1 binding, we performed mutation analysis of VuNAR1BM and tested VuNAR1 binding to the mutated sequences by yeast one-hybrid assays (Figure 7d). We found that VuNAR1 could interact with P5a that contains the original VuNAR1BM. However, when VuNAR1BM was fully mutated (P5aM), it prevents binding of VuNAR1. Point mutation analysis revealed that the second (A) of VuNAR1BM plays pivotal role in binding of VuNAR1, and mutation of other nucleotides did not significantly reduce the interaction. These results suggest that VuNAR1BM might be essential for the DNA binding of VuNAR1 *in vivo*.

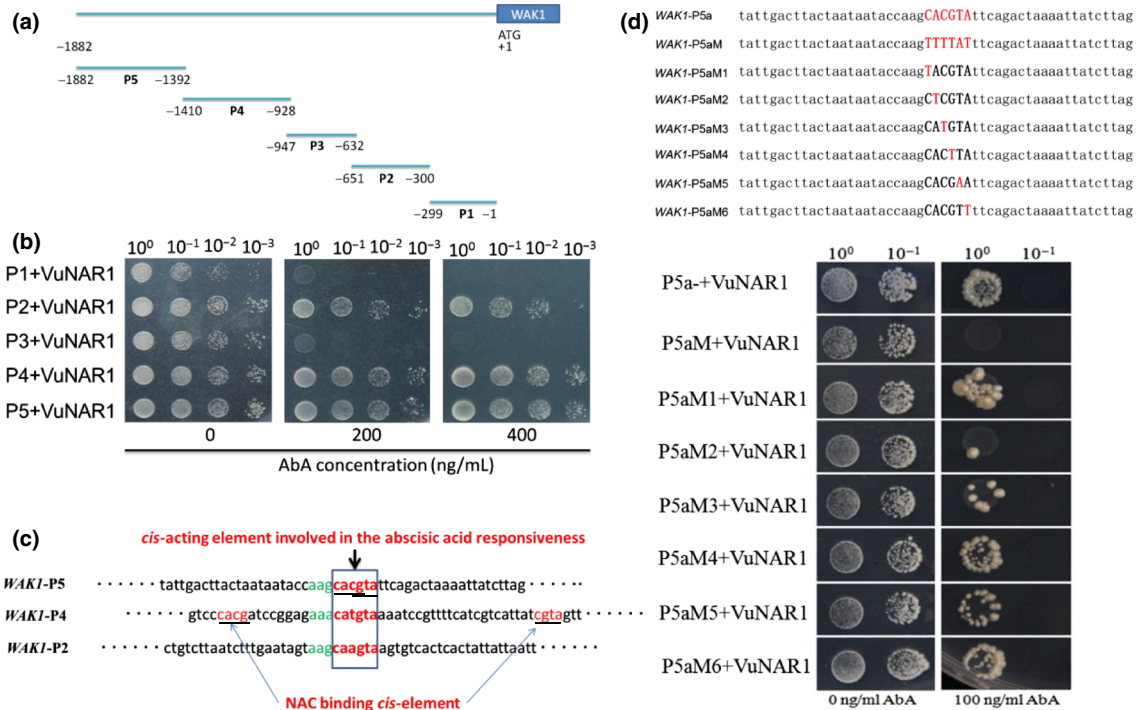


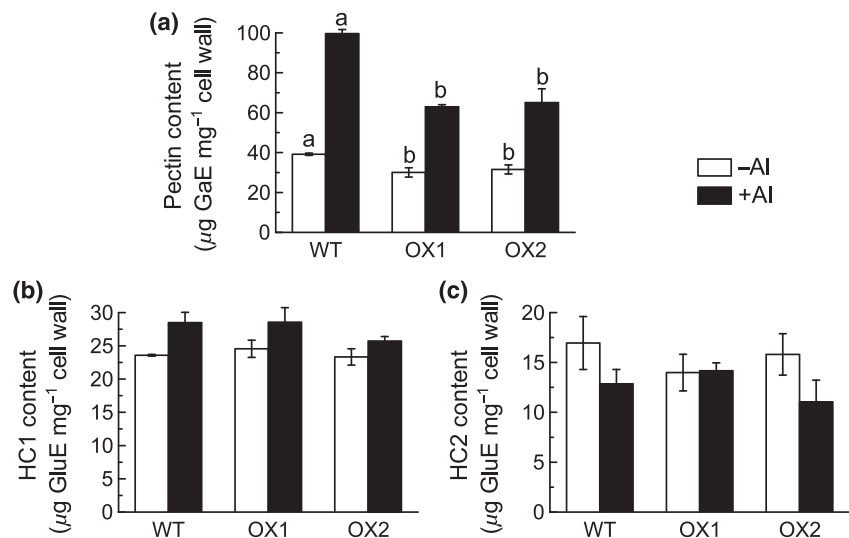
FIGURE 7 VuNAR1 activates WAK1 by binding to an ABRE-like motif. (a) Schematic diagram of the bait fragments (P1 to P5) used to construct the reporter vectors in the yeast one-hybrid assay. (b) Yeast one-hybrid assay. A pair of plasmids, pAbAi containing different fragments of WAK1 promoter and pGADT7 containing VuNAR1 were introduced into yeast strain Y1H gold and cultured on SD medium without Leu containing different concentrations of AbA at 30°C for 3 days. (c) Conserved sequence analysis using MEME motif discovery tool. (d) Interaction of VuNAR1 with VuNAR1BM and its mutated sequences in yeast one-hybrid assays. AbA, Aureobasidin A

In order to verify whether a similar mechanism operates in rice bean, we identified a WAK1-like gene in rice bean (*VuWAKL1*) based on our RNA-seq analysis of rice bean (Fan et al., 2019). Amino acid sequence alignment analysis showed that *VuWAKL1* contains a conserved protein kinase domain and shares 45% amino acid identity to *Arabidopsis* WAK1 (Figure S7). qRT-PCR analysis showed that the expression of *VuWAKL1* was significantly induced by half hour of Al treatment, and increased with exposure time within 12 hr (Figure S8). Next, we isolated a 735-bp length of *VuWAKL1* promoter sequence upstream of *VuWAKL1* translation start codon. We identified a ABRE-like motif and some NAC binding sites (NACBS, CGT(G/A)) in a 200-bp length of promoter sequence (Pro1, -2 to -202) of *VuWAKL1* (Figure S9). The result of yeast one-hybrid showed that *VuNAR1* could bind to the Pro1 to activate *AUR1-C* expression in yeast (Figure S10). These results suggested that *VuNAR1* could regulate Al resistance by directly binding to the promoter of *VuWAKL1* and induce its expression in rice bean.

3.8 | Cell wall pectin contributes to *VuNAR1*-mediated Al resistance

The GO clusterization of cell wall-associated genes that were specifically downregulated by *VuNAR1* suggests that WAK1 may regulate Al resistance through cell wall modification. To test this, we analysed cell wall polysaccharides as they are proved to be important for Al resistance (Horst, Wang, & Eticha, 2010). We found that Al exposure significantly increased pectin content of roots for all genotypes. Interestingly, the pectin content of roots was more abundant in WT than in the two OX1 and OX2 transgenic lines either in the absence or presence of Al (Figure 8a). By contrast, Al exposure did not significantly affect both hemicellulose 1 (Figure 8b) and hemicellulose 2 (Figure 8c) content of roots for all genotypes. Interestingly, the root pectin content of *wak1* mutants was significantly higher than WT plants (Figure S11).

FIGURE 8 Differential expression of *WAK1* is associated with cell wall polysaccharides content. (a) Pectin content. (b) Hemicellulose 1 content. (c) Hemicellulose 2 content. Two-week-old seedlings were exposed to one-fifth Hoagland solution (pH 5.0 without P) containing 0 or 25 μ M Al for 8 hr. Data are means \pm SD ($n = 4$). Bars with different letters are significantly different between genotypes at $p < .05$



4 | DISCUSSION

We demonstrated that a rice bean NAC-type TF, *VuNAR1*, is involved in Al resistance. Several lines of evidence support our current opinion. First, the expression of *VuNAR1* was rapidly induced by Al and the induction was dose dependent (Figure 1). Both low pH and other metals failed to induce *VuNAR1* expression (Figure 1), suggesting the expression specificity of *VuNAR1* to Al stress. Second, the expression induction was confined to root tip that is the primary target region of Al toxicity (Figure 1). Although Al-inducible expression of *VuNAR1* was observed at both root tip and basal root region, it is consistent with some suggestions that basal root region shares common Al resistance mechanisms with root tip region (Tsutsui et al., 2012; Zhu et al., 2015). Finally, overexpressing *VuNAR1* in *Arabidopsis* resulted in improved Al resistance (Figure 3).

We further demonstrated that external exclusion mechanism is related to *VuNAR1*-mediated Al resistance in *Arabidopsis*. This is evidenced by the lower Al content in transgenic *Arabidopsis* plants (Figure 3). The conclusion is also supported by the GO cellular component analysis, showing that the most significantly enriched GO cellular component is intracellular component in WT plant, while that is cell wall in OX plants (Figure 5B; Table S2). To date, STOP1-mediated transcriptional regulation of Al resistance genes represents the most well-documented Al resistance mechanism in plants (Delhaize et al., 2012; Kochian et al., 2015; Yang et al., 2019). However, we found that *VuNAR1*-improved Al resistance is not associated with these mechanisms. qRT-PCR analysis suggest that neither the expression of *STOP1* nor both *AtALMT1* and *AtMATE* differs between *VuNAR1* overexpressing lines and WT plants (Figure 4b). Furthermore, there were no significant differences between *VuNAR1ox* lines and WT plants with respect to other TF genes that positively regulate *AtALMT1* expression (Figure 4a), ruling out the possibility that *VuNAR1* facilitates Al exclusion via regulating organic acid anions secretion. Additionally, the expression of both *AtSTAR1* and *ALS3* as well as other STOP1-regulated genes were similarly regulated by Al between OX plants and WT plants (Figure 4c; Table S2).

Therefore, VuNAR1 provided another layer of regulatory control over AI stress responses.

Our comparative RNA-seq analysis revealed that the expression of 110 genes may be directly related to VuNAR1 under AI stress (Figure 5 a). NAC TFs act as either transcriptional activators or repressors in plant growth and development, hormone signalling, and stress responses (Hao et al., 2010; Lu et al., 2007; Olsen, Ernst, Leggio, & Skriver, 2005). VuNAR1 encodes a nuclear-localized NAC-type DNA-binding protein, and has transcriptional activation potential (Figure 2). Thus, the genes downregulated by VuANR1 may be the consequences of VuNAR1-regulated gene expression under AI stress. However, we cannot rule out the possibility that VuNAR1 directly suppresses these genes, which should be clarified in the future. GOBP analysis revealed that biological process of protein phosphorylation was most significantly enriched among differential expressed gene specifically upregulated by VuNAR1 (Figure 5c), by which the expression of *WAK1* was directly induced (Figure 5d). This conclusion was further confirmed by transient transcriptional regulation assays in tobacco leaves and in yeast cells (Figures 6 and 7). Sivaguru et al. (2003) reported that overexpression of *WAK1* could improve AI resistance in *Arabidopsis*. Here, we found that T-DNA insertion mutant plants, *wak1*, showed decreased resistance to AI stress (Figure S5). What is more, VuNAR1 could also bind to the promoter of *VuWAKL1* (Figure S10), presumably contributing to the transcriptional activation of *VuWAKL1* in rice bean (Figure S8). Therefore, we suggest that VuNAR1 enhances AI resistance by directly regulating *WAK1* expression.

NAC TFs typically recognize the conserved NACRS (Simpson et al., 2003; Tran et al., 2004). Unexpectedly, we found that VuNAR1 bound to DNA sequence either having or lacking NACRS (Figure 7). In this study, we used yeast one-hybrid assays and MEME motif discovery programme to identify the VuNAR1BM that has some sequence similarity to an ABA responsive *cis*-element. Similarly, Xu et al. (2013) demonstrated that ANAC096 specifically binds to the ABA-responsive element in the promoters of several drought stress-responsive genes. Notably, VuNAR1BM shares some sequence similarity with the conserved NACRS (Figure 5c). For example, ABA responsive *cis*-element in both P4 and P5 DNA sequence contain the CACG and CGTA motifs. Although P2 DNA sequence does not have the conserved NACRS, it contains CAAG motif. Our mutation analysis showed that only the second nucleotide in the VuNAR1BM is most essential for the binding activity of VuNAR1 (Figure 7d). Thus, it is likely that VuNAR1 can bind to both NACRS and ABA responsive *cis*-element. In line with our results, recent studies have reported that NAC can bind to different NAC binding motifs that do not harbour the CACG/CGTA core sequence (Sakuraba, Kim, Han, Lee, & Paek, 2015; Wu et al., 2012).

It is not surprising that *WAK1* promoter contains several ABA responsive *cis*-elements because *WAK1* expression has been suggested to be regulated by ABA (Sivaguru et al., 2003). It has been reported that some NACs can act either upstream or downstream of ABA to regulate gene expression. For example, NAC TFs such as VNI2 (Yang et al., 2011a), SNAC-As (Takasaki et al., 2015), ORE1 (Kim, Chung, & Woo, 2011), and OsNAP (Liang et al., 2014) are greatly upregulated by ABA. However, OsNAC2 can upregulate the

expression of ABA biosynthetic genes (OsNCED3 and OsZEP1) and downregulate the ABA catabolic gene (Miao et al., 2017). We found that the expression of *VuNAR1* can be induced by ABA treatment and AI stress rapidly induced ABA accumulation in root apex of rice bean (Fan et al., 2019). Therefore, it is reasonable to deduce that ABA may act upstream of *VuNAR1* to induce *WAK1* expression. The finding that *VuNAR1* may directly bind to the promoters of both *WAK1* and *VuWAKL1* and induces their expression supports this supposition. However, future work is required to clarify this.

It is, however, interesting to note that *VuNAR1* is not a functional homologue of *Arabidopsis* ATAF1, though ATAF1 is the closest homologue of *VuNAR1* in *Arabidopsis* (Figure S1). Consistent with previous report (Wu et al., 2009), overexpressing ATAF1 resulted in suppressed root growth (Figure S5). However, overexpressing *VuANR1* had opposite effects on root growth in comparison with ATAF1 (Figure S5). Furthermore, although ectopic expression of *VuNAR1* resulted in increased AI resistance, overexpression of ATAF1 did not (Figure S5). In addition, *ataf1* mutant plants did not show increased sensitivity to AI in comparison with WT plants (Figure S5). Given that ectopic expression of *VuNAR1* induced *WAK1* expression, question then arises as to how the expression of *WAK1* was regulated, because AI stress induced its expression in WT plants (Figure 5d; Sivaguru et al., 2003). We suggest two possibilities. First, there are more than 100 NAC TFs in *Arabidopsis* genome and sequence homology is insufficient for determining their physiological roles and transcriptional specificities. The activation potential of *VuNAR1* is possibly attributed to the high transcriptional activation activity of its C-terminal domain (Figure 2), which actually varied between *VuNAR1* and ATAF1. Therefore, it is other NAC TFs but not ATAF1 that regulate *WAK1* expression under AI stress. Second, NAC TFs form heterodimers with other TFs to synergistically or antagonistically regulate target gene expression. For example, the interaction of ANAC096 with two bZIP-type TFs, ABF2, and ABF4, resulted in the synergistic activation of the common target *RD29A*. However, ANAC019 could suppress ABF2-mediated *RD29A* (Xu et al., 2013). Therefore, *VuNAR1* may interact with unidentified TFs to synergistically induce *WAK1* expression.

One intriguing finding is that *WAK1* expression is associated with cell wall pectin content, which contributes to AI resistance. Although *wak1* exhibited increased AI sensitivity, transgenic lines overexpressing *VuNAR1* by which *WAK1* expression was greatly induced showed increased AI resistance. A recent study also suggests that the increased AI resistance in *Atgrp3* mutant might be related to the increase of *WAK1* free of AtGRP3 (Mangeon et al., 2015). Interestingly, such different expression levels of *WAK1* were positively correlated with cell wall pectin content but not with hemicelluloses content (Figures 8 and Figure S11). WAKs are receptor-like kinases that are linked to the pectin fraction of the cell wall (Kohorn & Kohorn, 2012). Although overexpression of *VuNAR1* upregulated *WAK1*, it affected the expression of genes associated with cell wall organization (Figure 5c), providing circumstantial evidence that *WAK1* affects metabolism of cell walls. Therefore, it is not surprising that *WAK1* expression affects pectin content. However, it remains unknown how *WAK1* regulates pectin metabolism, which requires further

investigation. Accumulating evidence suggests that cell wall pectin plays important roles in the expression of plant responses to Al toxicity (Horst et al., 2010). Previous reports also suggest that binding of Al with pectin resulted in the root growth inhibition in rice (Yang et al., 2008, 2013), *Arabidopsis* (Geng et al., 2017), and maize (Eticha et al., 2005). Thus, we suggest that VuNAR1 regulates Al resistance by regulating cell wall pectin metabolism via directly binding to the promoter of WAK1 and induce its expression.

ACCESSION NUMBERS

Sequence data from this article can be found in the GenBank/EMBL data libraries under the following accession numbers: VuNAR1 (MG256389), ATAF1 (AT1G01720), WAK1 (AT1G21250).

ACKNOWLEDGMENTS

This work was supported financially by the Natural Science Foundation of China (31222049; 31501827), the Chang Jiang Scholars Program (J.L.Y.), and 111 Project.

CONFLICT OF INTEREST

The authors declare that the research was conducted in the absence of any commercial or financial relationships that could be construed as a potential conflict of interest.

AUTHOR CONTRIBUTIONS

J.L.Y. and S.J.Z. planned and designed the research. H.Q.L., W.F., and J.F.J. performed experiments. J.M.X. and W.W.C. provided technical assistance to H.Q.L. J.L.Y. and H.Q.L. analysed data. J.L.Y. wrote the manuscript.

ORCID

He Qiang Lou  <https://orcid.org/0000-0002-2454-098X>

Jian Li Yang  <https://orcid.org/0000-0003-0385-5787>

Shao Jian Zheng  <https://orcid.org/0000-0002-3336-8165>

REFERENCES

- Bindea, G., Mlecnik, B., Hackl, H., Charoentong, P., Tosolini, M., Kirilovsky, A., ... Galon, J. (2009). ClueGO: A Cytoscape plug-in to decipher functionally grouped gene ontology and pathway annotation networks. *Bioinformatics*, 25, 1091–1093. <https://doi.org/10.1093/bioinformatics/btp101>
- Blumenkrantz, N., & Asboe-Hansen, G. (1973). New method for quantitative determination of uronic acids. *Analytical Biochemistry*, 54, 484–489. [https://doi.org/10.1016/0003-2697\(73\)90377-1](https://doi.org/10.1016/0003-2697(73)90377-1)
- Chai, M., Bellizzi, M., Wan, C., Cui, Z., Li, Y., & Wang, G. L. (2015). The NAC transcription factor OsSWN1 regulates secondary cell wall development in *Oryza sativa*. *Journal of Plant Biology*, 58, 44–51.
- Clough, S. J., & Bent, A. F. (1998). Floral dip: A simplified method for Agrobacterium-mediated transformation of *Arabidopsis thaliana*. *The Plant Journal*, 16, 735–743. <https://doi.org/10.1046/j.1365-313x.1998.00343.x>
- Cosgrove, D. J. (2005). Growth of the plant cell wall. *Nature Reviews Molecular Cell Biology*, 6, 850–861. <https://doi.org/10.1038/nrm1746>
- Decreux, A., & Messiaen, J. (2005). Wall-associated kinase WAK1 interacts with cell wall pectins in a calcium-induced conformation. *Plant and Cell Physiology*, 46, 268–278. <https://doi.org/10.1093/pcp/pci026>
- Delhaize, E., Ma, J. F., & Ryan, P. R. (2012). Transcriptional regulation of aluminium tolerance genes. *Trends in Plant Science*, 17, 341–348. <https://doi.org/10.1016/j.tplants.2012.02.008>
- Dong, J., Piñeros, M. A., Li, X., Yang, H., Liu, Y., Murphy, A. S., ... Liu, D. (2017). An *Arabidopsis* ABC transporter mediates phosphate deficiency-induced remodeling of root architecture by modulating iron homeostasis in roots. *Molecular Plant*, 10, 244–259. <https://doi.org/10.1016/j.molp.2016.11.001>
- Eticha, D., Stass, A., & Horst, W. J. (2005). Cell-wall pectin and its degree of methylation in the maize root-apex: Significance for genotypic differences in aluminium resistance. *Plant, Cell & Environment*, 28, 1410–1420.
- Fan, W., Lou, H. Q., Gong, Y. L., Liu, M. Y., Cao, M. J., Liu, Y., ... Zheng, S. J. (2015). Characterization of an inducible C2H2-type zinc finger transcription factor VuSTOP1 in rice bean (*Vigna umbellata*) reveals differential regulation between low pH and aluminum tolerance mechanisms. *New Phytologist*, 208, 456–468. <https://doi.org/10.1111/nph.13456>
- Fan, W., Lou, H. Q., Gong, Y. L., Liu, M. Y., Wang, Z. Q., Yang, J. L., & Zheng, S. J. (2014). Identification of early Al-responsive genes in rice bean (*Vigna umbellata*) roots provides new clues to molecular mechanisms of Al toxicity and tolerance. *Plant, Cell & Environment*, 37, 1586–1597.
- Fan, W., Xu, J. M., Wu, P., Yang, Z. X., Lou, H. Q., Chen, W. W., ... Yang, J. L. (2019). Alleviation by abscisic acid of Al toxicity in rice bean is not associated with citrate efflux but depends on ABI5-mediated signal transduction pathways. *Journal of Integrative Plant Biology*, 61, 140–154. <https://doi.org/10.1111/jipb.12695>
- Geng, X., Horst, W. J., Golz, J. F., Lee, J. E., Ding, Z., & Yang, Z. B. (2017). LEUNIG_HOMOLOG transcriptional co-repressor mediates aluminium sensitivity through PECTIN METHYLESTERASE46-modulated root cell wall pectin methylesterification in *Arabidopsis*. *The Plant Journal*, 90, 491–504. <https://doi.org/10.1111/tpj.13506>
- Hao, Y. J., Song, Q. X., Chen, H. W., Zou, H. F., Wei, W., Kang, X. S., ... Chen, S. Y. (2010). Plant NAC-type transcription factor proteins contain a NARD domain for repression of transcriptional activation. *Planta*, 232, 1033–1043. <https://doi.org/10.1007/s00425-010-1238-2>
- Horst, W. J., Schmohl, N., Kollmeier, M., & Sivaguru, M. (1999). Does aluminium affect root growth of maize through interaction with the cell wall-plasma membrane-cytoskeleton continuum? *Plant and Soil*, 215, 163–174.
- Horst, W. J., Wang, Y., & Eticha, D. (2010). The role of the root apoplast in aluminium-induced inhibition of root elongation and in aluminium resistance of plants: a review. *Annals of Botany*, 106, 185–197. <https://doi.org/10.1093/aob/mcq053>
- Huang, C. F., Yamaji, N., Chen, Z., & Ma, J. F. (2012). A tonoplast-localized half-size ABC transporter is required for internal detoxification of aluminum in rice. *The Plant Journal*, 69, 857–867. <https://doi.org/10.1111/j.1365-313X.2011.04837.x>
- Huang, C. F., Yamaji, N., & Ma, J. F. (2010). Knockout of a bacterial-type ATP-binding cassette transporter gene, AtSTAR1, results in increased aluminum sensitivity in *Arabidopsis*. *Plant Physiology*, 153, 1669–1677. <https://doi.org/10.1104/pp.110.155028>
- Huang, C. F., Yamaji, N., Mitani, N., Yano, M., Nagamura, Y., & Ma, J. F. (2009). A bacterial-type ABC transporter is involved in aluminum tolerance in rice. *Plant Cell*, 21, 655–667. <https://doi.org/10.1105/tpc.108.064543>
- Huang, W., Sherman, B. T., & Lempicki, R. A. (2009). Systematic and integrative analysis of large gene lists using DAVID bioinformatics resources. *Nature Protocols*, 4, 44–57.

- Hussey, S. G., Mizrahi, E., Creux, N. M., & Myburg, A. A. (2013). Navigating the transcriptional roadmap regulating plant secondary cell wall deposition. *Frontiers in Plant Science*, 4, 325.
- Iuchi, S., Koyama, H., Iuchi, A., Kobayashi, Y., Kitabayashi, S., Kobayashi, Y., ... Kobayashi, M. (2007). Zinc finger protein STOP1 is critical for proton tolerance in *Arabidopsis* and coregulates a key gene in aluminum tolerance. *Proceedings of the National Academy of Sciences of the United States of America*, 104, 9900–9905. <https://doi.org/10.1073/pnas.0700117104>
- Jefferson, R. A., Kavanagh, T. A., & Bevan, M. W. (1987). GUS fusions: Beta-glucuronidase as a sensitive and versatile gene fusion marker in higher plants. *EMBO Journal*, 6, 3901–3907.
- Kim, H. J., Chung, K. M., & Woo, H. R. (2011). Three positive regulators of leaf senescence in *Arabidopsis*, ORE1, ORE3 and ORE9, play roles in crosstalk among multiple hormone-mediated senescence pathways. *Genes & Genomics*, 33, 373–381.
- Kobayashi, Y., Ohyama, Y., Kobayashi, Y., Ito, H., Iuchi, S., Fujita, M., ... Koyama, H. (2014). STOP2 activates transcription of several genes for Al- and low pH tolerance that are regulated by STOP1 in *Arabidopsis*. *Molecular Plant*, 7, 311–322. <https://doi.org/10.1093/mp/ss116>
- Kochian, L. V. (1995). Cellular mechanisms of aluminum toxicity and resistance in plants. *Annual Review of Plant Physiology and Plant Molecular Biology*, 46, 237–260.
- Kochian, L. V., Piñeros, M. A., Liu, J., & Magalhaes, J. V. (2015). Plant adaptation to acid soils: The molecular basis for crop aluminum resistance. *Annual Review of Plant Biology*, 66, 571–598. <https://doi.org/10.1146/annurev-arplant-043014-114822>
- Kohorn, B. D., & Kohorn, S. L. (2012). The cell wall-associated kinases, WAKs, as pectin receptors. *Frontiers in Plant Science*, 3, 88.
- Larsen, P. B., Cancel, J., Rounds, M., & Ochoa, V. (2007). *Arabidopsis* ALS1 encodes a root tip and stele localized half type ABC transporter required for root growth in an aluminum toxic environment. *Planta*, 225, 1447–1458. <https://doi.org/10.1007/s00425-006-0452-4>
- Larsen, P. B., Geisler, M. J. B., Jones, C. A., Williams, K. M., & Cancel, J. D. (2005). ALS3 encodes a phloem-localized ABC transporter-like protein that is required for aluminum tolerance in *Arabidopsis*. *The Plant Journal*, 41, 353–363. <https://doi.org/10.1111/j.1365-313X.2004.02306.x>
- Li, R., Yu, C., Li, Y., Lam, T. W., Yiu, S. M., Kristiansen, K., & Wang, J. (2009). SOAP2: An improved ultrafast tool for short read alignment. *Bioinformatics*, 25, 1966–1967. <https://doi.org/10.1093/bioinformatics/btp336>
- Liang, C., Wang, Y., Zhu, Y., Tang, J., Hu, B., Liu, L., ... Chu, J. (2014). OsNAP connects abscisic acid and leaf senescence by fine-tuning abscisic acid biosynthesis and directly targeting senescence-associated genes in rice. *Proceedings of the National Academy of Sciences of the United States of America*, 111, 10013–10018. <https://doi.org/10.1073/pnas.1321568111>
- Liu, J., Magalhaes, J. V., Shaff, J., & Kochian, L. V. (2009). Aluminum-activated citrate and malate transporters from the MATE and ALMT families function independently to confer *Arabidopsis* aluminum tolerance. *The Plant Journal*, 57, 389–399. <https://doi.org/10.1111/j.1365-313X.2008.03696.x>
- Liu, M. Y., Chen, W. W., Xu, J. M., Fan, W., Yang, J. L., & Zheng, S. J. (2013). The role of VuMATE1 expression in aluminium-inducible citrate secretion in rice bean (*Vigna umbellata*) roots. *Journal of Experimental Botany*, 64, 1795–1804. <https://doi.org/10.1093/jxb/ert039>
- Lu, P. L., Chen, N. Z., An, R., Su, Z., Qi, B. S., Ren, F., ... Wang, X. C. (2007). A novel drought-inducible gene, ATAF1, encodes a NAC family protein that negatively regulates the expression of stress responsive genes in *Arabidopsis*. *Plant Molecular Biology*, 63, 289–305. <https://doi.org/10.1007/s11103-006-9089-8>
- Ma, J. F. (2007). Syndrome of aluminum toxicity and diversity of aluminum resistance in higher plants. *International Review of Cytology*, 264, 225–253.
- Mangeon, A., Pardal, R., Menezes-Salgueiro, A. D., Duarte, G. L., de Seixas, R., Cruz, F. P., ... Sachetto-Martins, G. (2015). AtGRP3 is implicated in root size and aluminum response pathways in *Arabidopsis*. *PLoS ONE*, 11, e0150583.
- Miao, C., Lu, S., Lv, B., Zhang, B., Shen, J., He, J., ... Ming, F. (2017). A rice NAC transcription factor promotes leaf senescence via ABA biosynthesis. *Plant Physiology*, 174, 1747–1763. <https://doi.org/10.1104/pp.17.00542>
- Mitsuda, N., Iwase, A., Yamamoto, H., Yoshida, M., Seki, M., Shinozaki, K., & Ohme-Takagi, M. (2007). NAC transcription factors, NST1 and NST3, are key regulators of the formation of secondary walls in woody tissues of *Arabidopsis*. *The Plant Cell*, 19, 270–280. <https://doi.org/10.1105/tpc.106.047043>
- Mitsuda, N., Seki, M., Shinozaki, K., & Ohme-Takagi, M. (2005). The NAC transcription factors NST1 and NST2 of *Arabidopsis* regulate secondary wall thickenings and are required for anther dehiscence. *The Plant Cell*, 17, 2993–3006. <https://doi.org/10.1105/tpc.105.036004>
- Mortazavi, A., Williams, B. A., McCue, K., Schaeffer, L., & Wold, B. (2008). Mapping and quantifying mammalian transcriptomes by RNA-seq. *Nature Methods*, 5, 621–628. <https://doi.org/10.1038/nmeth.1226>
- Nuruzzaman, M., Sharoni, A. M., & Kikuchi, S. (2013). Roles of NAC transcription factors in the regulation of biotic and abiotic stress responses in plants. *Frontiers in Microbiology*, 4, 248.
- Olsen, A. N., Ernst, H. A., Leggio, L. L., & Skriver, K. (2005). NAC transcription factors: Structurally distinct, functionally diverse. *Trends in Plant Science*, 10, 79–87. <https://doi.org/10.1016/j.tplants.2004.12.010>
- Ryan, P. R., Delhaize, E., & Jones, D. L. (2001). Function and mechanism of organic anion exudation from plant roots. *Annual Review of Plant Biology*, 52, 527–560.
- Sakuraba, Y., Kim, Y. S., Han, S. H., Lee, B. D., & Paek, N. C. (2015). The *Arabidopsis* transcription factor NAC016 promotes drought stress responses by repressing AREB1 transcription through a trifurcate feed-forward regulatory loop involving NAP. *The Plant Cell*, 27, 1771–1787. <https://doi.org/10.1105/tpc.15.00222>
- Shannon, P., Markiel, A., Ozier, O., Baliga, N. S., Wang, J. T., Ramage, D., ... Ideker, T. (2003). Cytoscape: A software environment for integrated models of biomolecular interaction networks. *Genome Research*, 13, 2498–2504. <https://doi.org/10.1101/gr.1239303>
- Simpson, S. D., Nakashima, K., Narusaka, Y., Seki, M., Shinozaki, K., & Yamaguchi-Shinozaki, K. (2003). Two different novel cis acting elements of erd1, a clpA homologous *Arabidopsis* gene function in induction by dehydration stress and dark-induced senescence. *The Plant Journal*, 33, 259–270. <https://doi.org/10.1046/j.1365-313x.2003.01624.x>
- Sivaguru, M., Ezaki, B., He, Z. H., Tong, H., Osawa, H., Baluska, F., ... Matsumoto, H. (2003). Aluminum-induced gene expression and protein localization of a cell wall-associated receptor kinase in *Arabidopsis*. *Plant Physiology*, 132, 2256–2266. <https://doi.org/10.1104/pp.103.022129>
- Takasaki, H., Maruyama, K., Takahashi, F., Fujita, M., Yoshida, T., Nakashima, K., ... Shinozaki, K. (2015). SNAC-As, stress-responsive NAC transcription factors, mediate ABA-inducible leaf senescence. *The Plant Journal*, 84, 1114–1123. <https://doi.org/10.1111/tpj.13067>
- Thirumalaikumar, V. P., Devkar, V., Mehterov, N., Ali, S., Ozgur, R., Turkan, I., ... Balazadeh, S. (2017). NAC transcription factor JUNGBRUNNEN1 enhances drought tolerance in tomato. *Plant Biotechnology Journal*, 16, 354–366.
- Tokizawa, M., Kobayashi, Y., Saito, T., Kobayashi, M., Iuchi, S., Nomoto, M., ... Koyama, H. (2015). Sensitive to proton rhizotoxicity1, calmodulin

- binding transcription activator2, and other transcription factors are involved in *aluminum-activated malate transporter1* expression. *Plant Physiology*, 167, 991–1003. <https://doi.org/10.1104/pp.114.256552>
- Tran, L. S., Nakashima, K., Sakuma, Y., Simpson, S. D., Fujita, Y., Maruyama, K., ... Yamaguchi-Shinozaki, K. (2004). Isolation and functional analysis of *Arabidopsis* stress-inducible NAC transcription factors that bind to a drought responsive cis-element in the early responsive to dehydration stress 1 promoter. *The Plant Cell*, 16, 2481–2498. <https://doi.org/10.1105/tpc.104.022699>
- Tsutsui, T., Yamaji, N., Huang, C. F., Motoyama, R., Nagamura, Y., & Ma, J. F. (2012). Comparative genome-wide transcriptional analysis of Al-responsive genes reveals novel Al tolerance mechanisms in rice. *PLoS ONE*, 7, e48197.
- Uexküll, H., & Mutert, E. (1995). Global extent, development and economic impact of acid soils. *Plant and Soil*, 171, 1–15.
- Wu, A., Allu, A. D., Garapati, P., Siddiqui, H., Dortay, H., Zanol, M. I., ... Balazadeh, S. (2012). JUNGBRUNNEN1, a reactive oxygen species responsive NAC transcription factor, regulates longevity in *Arabidopsis*. *The Plant Cell*, 24, 482–506. <https://doi.org/10.1105/tpc.111.090894>
- Wu, Y., Deng, Z., Lai, J., Zhang, Y., Yang, C., Yin, B., ... Xie, Q. (2009). Dual function of *Arabidopsis* ATAF1 in abiotic and biotic stress responses. *Cell Research*, 19, 1279–1290. <https://doi.org/10.1038/cr.2009.108>
- Wyatt, S. E., & Carpita, N. C. (1993). The plant cytoskeleton-cell wall continuum. *Trends in Cell Biology*, 3, 413–417. [https://doi.org/10.1016/0962-8924\(93\)90022-s](https://doi.org/10.1016/0962-8924(93)90022-s)
- Xia, J., Yamaji, N., Kasai, T., & Ma, J. F. (2010). Plasma membrane-localized transporter for aluminum in rice. *Proceedings of the National Academy of Sciences*, 107, 18381–18385.
- Xu, J. M., Wang, Z. Q., Jin, J. F., Chen, W. W., Fan, W., Zheng, S. J., & Yang, J. L. (2019). FeSTAR2 interacted by FeSTAR1 alters its subcellular location and regulates Al tolerance in buckwheat. *Plant and Soil*, 436, 489–501.
- Xu, Z. Y., Kin, S. Y., Hyeon, D. Y., Kim, D. H., Dong, T., ... Hwang, I. (2013). The *Arabidopsis* NAC transcription factor ANAC096 cooperates with bZIP-type transcription factors in dehydration and osmotic stress responses. *The Plant Cell*, 25, 4708–4724. <https://doi.org/10.1105/tpc.113.119099>
- Yamaguchi, M., & Demura, T. (2010). Transcriptional regulation of secondary wall formation controlled by NAC domain proteins. *Plant Biotechnology*, 27, 237–242.
- Yamaji, N., Huang, C. F., Nagao, S., Yano, M., Sato, Y., Nagamura, Y., & Ma, J. F. (2009). A zinc finger transcription factor ART1 regulates multiple genes implicated in aluminum tolerance in rice. *The Plant Cell*, 21, 3339–3349. <https://doi.org/10.1105/tpc.109.070771>
- Yang, J. L., Fan, W., & Zheng, S. J. (2019). Mechanisms and regulation of aluminum-induced secretion of organic acid anions from plant roots. *Journal of Zhejiang University-SCIENCE B*, 20, 513–527. <https://doi.org/10.1631/jzus.B1900188>
- Yang, J. L., Li, Y. Y., Zhang, Y. J., Zhang, S. S., Wu, Y. R., Wu, P., & Zheng, S. J. (2008). Cell wall polysaccharides are specifically involved in the exclusion of aluminum from the rice root apex. *Plant Physiology*, 146, 602–611. <https://doi.org/10.1104/pp.107.111989>
- Yang, J. L., Zhu, X. F., Peng, Y. X., Zheng, C., Li, G. X., Liu, Y., ... Zheng, S. J. (2011a). Cell wall hemicellulose contributes significantly to aluminum adsorption and root growth in *Arabidopsis*. *Plant Physiology*, 155, 1885–1892. <https://doi.org/10.1104/pp.111.172221>
- Yang, S. D., Seo, P. J., Yoon, H. K., & Park, C. M. (2011b). The *Arabidopsis* NAC transcription factor VNI2 integrates abscisic acid signals into leaf senescence via the COR/RD genes. *The Plant Cell*, 23, 2155–2168. <https://doi.org/10.1105/tpc.111.084913>
- Yang, X. Y., Zeng, Z. H., Yan, J. Y., Fan, W., Bian, H. W., Zhu, M. Y., ... Zheng, S. J. (2013). Association of specific pectin methylsterases with Al-induced root elongation inhibition in rice. *Physiology Plant*, 148, 502–511. <https://doi.org/10.1111/ppl.12005>
- Yoshida, K., Sakamoto, S., Kawai, T., Kobayashi, K., Sato, K., Ichinose, Y., ... Mitsuda, N. (2013). Engineering the *Oryza sativa* cell wall with rice NAC transcription factors regulating secondary wall formation. *Frontiers in Plant Science*, 4, 383.
- Zheng, S. J., & Yang, J. L. (2005). Target sites of aluminum phytotoxicity. *Biology Plant*, 49, 321–331.
- Zhong, R., Demura, T., & Ye, Z. H. (2006). SND1, a NAC domain transcription factor, is a key regulator of secondary wall synthesis in fibers of *Arabidopsis*. *The Plant Cell*, 18, 3158–3170. <https://doi.org/10.1105/tpc.106.047399>
- Zhong, R., Lee, C., McCarthy, R. L., Reeves, C. K., Jones, E. G., & Ye, Z. H. (2011). Transcriptional activation of secondary wall biosynthesis by rice and maize NAC and MYB transcription factors. *Plant and Cell Physiology*, 52, 1856–1871. <https://doi.org/10.1093/pcp/pcr123>
- Zhu, H., Wang, H., Zhu, Y., Zou, J., Zhao, F. J., & Huang, C. F. (2015). Genomewide transcriptomic and phylogenetic analyses reveal distinct aluminum tolerance mechanisms in the aluminum-accumulating species buckwheat (*Fagopyrum tataricum*). *BMC Plant Biology*, 15, 16.
- Zhu, X. F., Shi, Y. Z., Lei, G. J., Fry, S. C., Zhang, B. C., Zhou, Y. H., ... Zheng, S. J. (2012). XTH31, encoding an in vitro XEH/XET-active enzyme, regulates aluminum sensitivity by modulating in vivo XET action, cell wall xyloglucan content, and aluminum binding capacity in *Arabidopsis*. *The Plant Cell*, 24, 4731–4747. <https://doi.org/10.1105/tpc.112.106039>
- Zhu, X. F., Wan, J. X., Sun, Y. Z., Braam, J., Li, G. X., & Zheng, S. J. (2014). Xyloglucan endotransglucosylase-hydrolase17 interacts with xyloglucan endotransglucosylase-hydrolase31 to confer xyloglucan endotransglucosylase action and affect aluminum sensitivity in *Arabidopsis*. *Plant Physiology*, 165, 1566–1574. <https://doi.org/10.1104/pp.114.243790>

SUPPORTING INFORMATION

Additional supporting information may be found online in the Supporting Information section at the end of the article.

Figure S1. Sequence alignment and phylogenetic relationship of VuNAR1.

Figure S2. The sequence of VuNAR1 promoter.

Figure S3. Al visualization by morin staining.

Figure S4. ATAF1 expression analysis.

Figure S5. Comparison of differential Al resistance among WT, *ataf1*, *wak1*, VuNAR1 overexpression line (NARox1), and ATAF1 overexpression lines (ATAFox1).

Figure S6. Correlation of gene expression levels between RNA-seq data and qRT-PCR analysis.

Figure S7. Amino acid sequence alignment of VuWAKL1 from rice bean with the WAK1 from *Arabidopsis*.

Figure S8. Expression of VuWAKL1 in rice bean root apices (0–1 cm) in response to 25 μ M Al for different times.

Figure S9. The sequence of VuWAKL1 promoter.

Figure S10. VuNAR1 binds to the promoter of VuWAKL1.

Figure S11. Pectin content in Col-0 (WT) and *wak1* lines.

TABLE S1. Primers used in this study.

TABLE S2. RNA-seq analysis.

How to cite this article: Lou HQ, Fan W, Jin JF, et al. A NAC-type transcription factor confers aluminium resistance by regulating cell wall-associated receptor kinase 1 and cell wall pectin. *Plant Cell Environ.* 2020;43:463–478. <https://doi.org/10.1111/pce.13676>